Modified Cathodes with Carbon-Based Nanomaterials for Electro-Fenton Process

Alireza Khataee and Aliyeh Hasanzadeh

Abstract Electro-Fenton (EF) process is based on the continuous in situ production of hydrogen peroxide (H_2O_2) by a two-electron reduction of oxygen on cathode and the addition of ferrous ion to generate hydroxyl radical ($^{\bullet}OH$) at the solution through Fenton's reaction in acidic condition. Hence, cathode material has prominent effects on the H_2O_2 electro-generation efficiency and regeneration of ferrous ion. Carbonaceous materials are applied as suitable cathode in virtue of being highly conductive, stable, nontoxic, and commercially available. Besides, modification of cathode electrode with carbon-based nanomaterials (e.g., carbon nanotubes (CNTs), graphene, mesoporous carbon) can improve the electroactive surface area and the rate of oxygen mass transfer to the electrode, which increases the H_2O_2 electro-generation in the EF process. This chapter is to summarize the recent progress and advances in the modification of cathode electrode with carbon-based nanomaterials for EF process. The ability of different carbon-based nanomaterials to electro-generate H_2O_2 and degradation of pollutants is also discussed briefly.

Keywords Carbon nanomaterials, Carbon nanotubes, Electro-Fenton, Graphene, Graphene oxide, Hydrogen peroxide, Mesoporous carbon, Reduced graphene oxide

Contents

A. Khataee (✉) and A. Hasanzadeh
Research Laboratory of Advanced Water and Wastewater Treatment Processes, Department of Applied Chemistry, Faculty of Chemistry, University of Tabriz, Tabriz, Iran
e-mail: a_khataee@tabrizu.ac.ir

M. Zhou et al. (eds.), *Electro-Fenton Process: New Trends and Scale-Up*,
Hdb Env Chem, DOI 10.1007/698_2017_74,

Abbreviations

ACF	Activated carbon fiber
AQS	Anthraquinone monosulfonate
BDD	Boron-doped diamond
CF	Carbon felt
CNT	Carbon nanotube
CTAB	Cetyl trimethyl ammonium bromide
DETA	3-(Trimethoxysilylpropyl) diethylenetriamine
EF	Electro-Fenton
ERGO	Electrochemical reduction of graphene oxide
GDE	Gas diffusion electrode
GO	Graphene oxide
HPC	Hierarchically porous carbon
MOF	Metal-organic framework
MWCNTs	Multiwalled carbon nanotubes
OMC	Ordered mesoporous carbons
PTFE	Polytetrafluoroethylene
rGO	Reduced graphene oxide
Rh B	Rhodamine B
RVC	Reticulated vitreous carbon
SEM	Scanning electron microscopy
SWNTs	Single-walled nanotubes
TEM	Transmission electron microscopy
TOC	Total organic carbon

1 Introduction

Electro-Fenton (EF) process is based on the continuous in situ production of hydrogen peroxide (H_2O_2) and the addition of Fe^{2+} ion as a catalyst to generate hydroxyl radical ($^{\bullet}OH$) at the solution through Fenton's reaction in acidic condition as the following reaction:

$$Fe^{2+} + H_2O_2 + H^+ \rightarrow Fe^{3+} + {}^{\bullet}OH + H_2O \quad (1)$$

H_2O_2 can be continuously produced in an electrolytic cell from the two-electron reduction of oxygen gas at the cathode electrode by reaction (2) ($E^{\circ} = 0.695$ V/SHE),

which occurs more easily than its four-electron reduction to water from reaction (3) ($E^\circ = 1.23$ V/SHE) [1]:

$$O_2(g) + 2H^+ + 2e^- \rightarrow H_2O_2 \quad (2)$$

$$O_2(g) + 4H^+ + 4e^- \rightarrow 2H_2O \quad (3)$$

In EF process, Fe^{2+} can be regenerated via cathodic reduction (reaction (4)), which accelerates the generation of $^{\bullet}OH$ from Fenton's reaction (1):

$$Fe^{3+} + e^- \rightarrow Fe^{2+} \quad (4)$$

Cathode material has prominent effects on the oxidation power of the EF process and H_2O_2 electro-generation efficiency. Carbonaceous materials are subject of great interest as cathode electrodes for the two-electron reduction of O_2 to H_2O_2 and the favorable options for electrocatalyst support in virtue of being nontoxic and stable and having high overpotential for H_2 evolution and relatively good chemical resistance and conductivity [2]. In the 1970s, Oloman and Watkinson [3, 4] firstly investigated the application of graphite particles in the trickle-bed electrochemical reactors for the cathodic reduction of O_2 to H_2O_2. Especially worth noting are the researches reporting the use of planar (2D) cathodes such as graphite [5–9], gas diffusion electrodes (GDEs) [10–13], three-dimensional (3D) electrodes such as activated carbon fiber (ACF) [14], carbon felt (CF) [15–19], carbon sponge [20, 21], reticulated vitreous carbon (RVC) [22–24], O_2-fed carbon polytetrafluoroethylene (PTFE) [25, 26], and boron-doped diamond (BDD) [27, 28].

Due to the poor solubility of O_2 in aqueous solution (about 40 or 8 mg L^{-1} in contact with pure O_2 or air, respectively, at 1 atm and 25°C), GDEs and 3D electrodes of high specific surface area are favored as cathodes to supply reasonable current densities for practical applications. GDEs have a thin and porous structure preferring the percolation of the injected gas across its pores to contact the solution at the carbon surface. These electrodes have a great amount of active surface sites leading to a very fast O_2 reduction and large production of H_2O_2 [1]. Figure 1 provides a schematic diagram of structure and function of GDE.

In the last three decades, carbon-based nanomaterials have attracted substantial attention due to their superior electronic, photonic, electrocatalytic, chemical, and mechanical features that remarkably depend on their nanoscale properties [29]. Carbon-based nanomaterials can be classified into two groups: nanosized and nanostructured carbons [30]. Many more types of carbon materials, including graphene family (e.g., graphene, graphene oxide (GO), and reduced graphene oxide (rGO)), carbon nanotubes (CNTs), nanofibers, nanodiamonds, nanocoils, nanoribbon, and fullerene belonging to nanosized class, because the shell size and thickness of these carbon materials are on the nanometer scale [29]. New carbon materials such as carbon fibers and ordered mesoporous carbons are classified as nanostructured carbons, because their nanostructure is controlled in their construction through various processes [30]. Figure 2 provides a schematic illustration of some nanocarbons. Carbon blacks are constructed of nanosized particles, but they

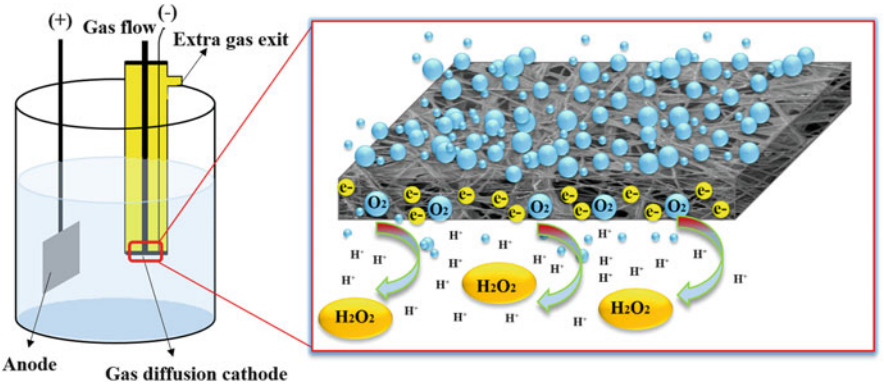

Fig. 1 Schematic diagram of structure and function of GDE

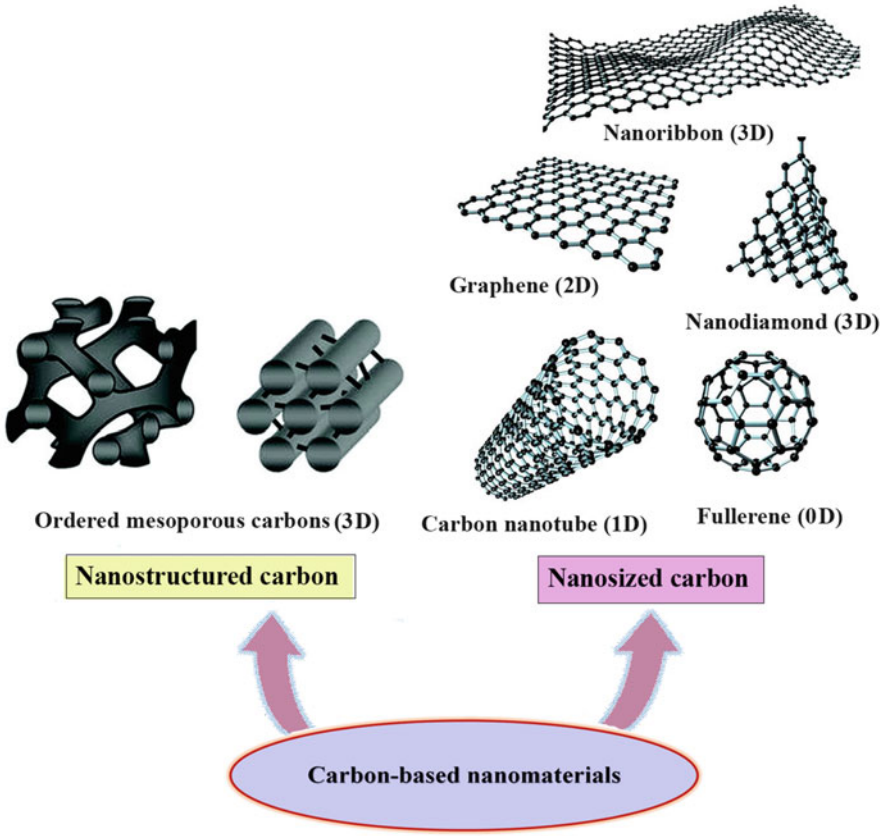

Fig. 2 Schematic illustration of some carbon-based nanomaterials

do not usually belong to nanocarbons due to their various applications as a mass and not in their distinctive form of nanosized particles [31].

In addition, doping carbon nanomaterials with heteroatoms, especially nitrogen, can enhance the performance of oxygen reduction activity by improving the surface chemical reactivity, conductivity, catalytic sites, and stability [32]. Among different possible dopants, nitrogen doping could either enhance the current of oxygen reduction or diminish the onset overpotential through (1) increasing chemically active sites, (2) improving the O_2 chemisorption, and (3) enhancing the hydrophilicity of surface [33].

Therefore, there are many investigations focused on the modification of cathode electrode by carbon-based nanomaterials [5, 34–36]. In these studies, the performance of EF process has been enhanced through improving the mass transfer characteristics of cathode. The novel EF electrode materials should possess several properties as follows: high selectivity for two-electron reduction of oxygen, good mass transfer performance, high electrochemical active reaction area, and high electrical conductivity.

The purpose of this chapter is to review the attempts in surface modification of cathode electrodes with carbon-based nanomaterials, e.g., CNTs, graphene family, and mesoporous carbons for EF process.

2 Modification of Cathodes with Carbon-Based Nanomaterials for EF Process

2.1 Carbon Nanotubes

The discovery of CNTs by Iijima in 1991 [37] has created a revolution in nanotechnology and material science. CNTs have attracted substantial consideration from the scientific community as one of the main members of carbon nanomaterials with unique optoelectronic, electrochemical, and electronic features [38]. The carbon atoms in CNTs are ordered in hexagons with sp^2 hybridization (one-dimensional (1D) system) [29]. A single-walled CNT (SWCNT) is produced by the rolling of a graphite layer into a nanoscale tube form which has an approximate diameter of 1 nm. Multiwalled CNTs (MWCNTs) can be constituted of two or more numbers of coaxial SWCNTs with expanding diameters that are separated from each other by a distance of around 0.34 nm (see Fig. 3) [33].

CNTs can be semiconducting or metallic in their electronic properties with an electrical conductivity up to 5,000 S cm^{-1} [38]. Their conductivity is highly dependent on their chirality of the graphitic hexagonal array and diameter. The highly conductive nature of the CNTs confirms their high charge transport ability [29]. Experimental specific surface area of SWCNTs is in the range between 370 and 1,587 m^2 g^{-1} with micropore volume of 0.15–0.3 cm^3 g^{-1} [39]. The MWCNT has a specific surface area between 180.9 and 507 m^2 g^{-1} with mesopore

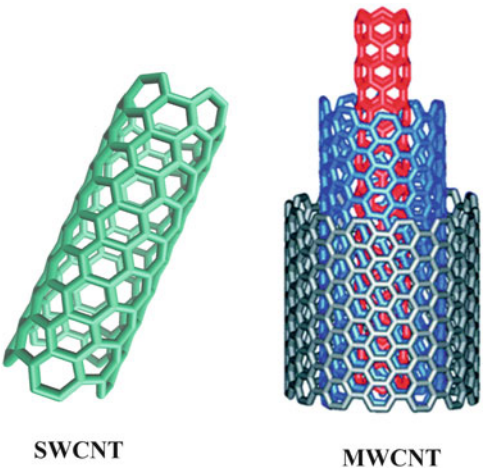

Fig. 3 The structure of SWCNT and MWCNT

volume of 0.5–2 $cm^3\ g^{-1}$ [39]. The tensile modulus and strength of SWCNTs are usually in the range of 320–1,740 GPa and 13–52 GPa, respectively, while being 270–950 GPa and 11–63 GPa in MWCNTs [29, 38]. Besides the huge specific surface area and electrical conductivity, CNTs also have a great thermal conductivity of 6,000 W mK^{-1} [38]. Due to these interesting properties, CNTs are promising nanomaterials for different applications such as in hydrogen-storage systems, sensors, organic photovoltaic cells, supercapacitors, fuel cells, batteries, and solar cells [29, 38, 39]. The applications of CNTs and their derivatives as electrocatalysts for two-electron reduction of O_2 in EF system will be discussed.

During the last years, a number of researches have been focused on the modification of cathode electrode with CNTs to improve its performance for in situ H_2O_2 generation in EF oxidation process. Table 1 summarizes some of the recent reported that modified cathode with CNTs and their derivatives in EF process.

Zarei et al. [52–54] coated the surface of carbon paper as a GDE cathode with CNTs and compared its efficiency for in situ H_2O_2 generation with activated carbon/GDE. PTFE was used to bind the carbon materials into a cohesive layer and convey some hydrophobic feature to the electrode surface. The scanning electron microscopy (SEM) images of the uncoated GDE and CNTs/GDE are shown in Fig. 4. As it can be seen from SEM images, coating of CNTs on GDE electrode improves the specific surface area of the cathode. The results demonstrated that the amount of produced H_2O_2 on the CNTs/GDE electrode (14.3 mmol L^{-1}) was approximately three times higher than that of activated carbon/GDE electrode (5.9 mmol L^{-1}) (Fig. 4c). The degradation efficiency of Basic Yellow 2 (BY2) in peroxi-coagulation process reached 62% and 96% in the first 10 min using activated carbon/GDE and CNTs/GDE electrodes at 100 mA, respectively [52]. The different abilities of H_2O_2 electro-generation of activated carbon/GDE and CNTs/GDE electrodes are attributed to the huge surface area and good electrical conductivity of CNTs [52–54].

Table 1 Selected results reported for modified cathodes with carbon nanotubes

Modified cathode	Process	Pollutant	Operational parameters	Maximum efficiency reported	Ref.
Oxidized MWCNT/GDE	EF	Methyl orange (MO)	250 mL reaction compartment, Pt wire anode, 0.05 mol L^{-1} Na_2SO_4 (electrolyte), pH 3.0, 400 mL min^{-1} O_2 flow rate, 0.2 mmol L^{-1} [Fe^{2+}], 1.0 V voltage	95% removal efficiency for 100 mg L^{-1} MO, 4.38 mmol L^{-1} [H_2O_2] after 90 min electrolysis and 81% current efficiency for CNT-15 (15 min plasma traded time)/GDE	[40]
MWCNT/graphite felt	EF	Rhodamine B (Rh B)	500 mL reaction compartment, 0.06 cm^2 Pt sheet anode, 0.05 mol L^{-1} [Na_2SO_4] (electrolyte), pH 3.0, 1,000 mL min^{-1} air flow rate, 0.5 mmol L^{-1} [Fe^{2+}], 5 mA cm^{-2} current density	98.49% removal efficiency for 50 mg L^{-1} Rh B and 9.58 mmol L^{-1} [H_2O_2] after 360 min electrolysis	[41]
PTFE@MWCNT	EF	*m*-cresol	200 mL reaction compartment, 38 cm^2 Ti/SnO_2–Sb_2O_5–IrO_2 anode, 0.1 mol L^{-1} [Na_2SO_4] (electrolyte), pH 3.0, 1,000 mL min^{-1} air flow rate, 0.4 mmol L^{-1} [Fe^{2+}], 2.9 mA cm^{-2} current density	99% removal efficiency for 100 mg L^{-1} *m*-cresol and 4.76 mmol L^{-1} [H_2O_2] after 150 min electrolysis	[42]
MWCNT/graphite	Photocatalytic-EF	AY36	1000 mL reaction compartment, 11.5 cm^2 Pt anode, 0.05 mol L^{-1} [Na_2SO_4] (electrolyte), pH 3.0, 2500 mL min^{-1} air flow rate, 0.1 mmol L^{-1} [Fe^{2+}], 2.7 mA cm^{-2} current density	82.24% removal efficiency for 20 mg L^{-1} AY36 and 0.12 mmol L^{-1} [H_2O_2] after 180 min electrolysis	[43]
MWCNT/GDE	Photo-EF	Acid Blue 5 (AB5)	2000 mL recirculation reactor with UV lamp, 1.0 cm^2 Pt anode, 0.05 mol L^{-1} [Na_2SO_4] (electrolyte), pH 3.0, 1000 mL min^{-1} solution flow rate, 0.2 mmol L^{-1} [Fe^{3+}], 2.9 mA cm^{-2} current density	23% and 98.25% removal efficiency of EF and photo-EF processes for 20 mg L^{-1} AB5, respectively, after 60 min reaction time	[44]
		Direct Red 23 (DR23)		94.29% removal efficiency for 30 mg L^{-1} DR23 (after 60 min reaction time)/c	[45]

(continued)

Table 1 (continued)

Modified cathode	Process	Pollutant	Operational parameters	Maximum efficiency reported	Ref.
MWCNT-surfactant/graphite	EF	Acid Red 14 (AR14) and Acid Blue 92 (AB92)	1000 mL continuous reactor, 26 cm^2 graphite anode, 0.05 mol L^{-1} [Na_2SO_4] (electrolyte), pH 3.0, 5.5 mL min^{-1} solution flow rate, 0.1 mmol L^{-1} [Fe^{3+}], 6.92 mA cm^{-2} current density	99% and 95% removal efficiency for 50 mg L^{-1} AR14 and AB92, respectively, after 220 min reaction time	[46]
	Heterogeneous-EF		250 mL reaction compartment, 26 cm^2 graphite anode, 0.05 mol L^{-1} [Na_2SO_4] and [NaCl] (electrolyte), pH 3.0, 1.0 g L^{-1} Fe_3O_4 NPs, 6.92 mA cm^{-2} current density	100% removal efficiency for 50 mg L^{-1} AR14 and AB92 in NaCl electrolyte solution after 120 min reaction time	[47]
Fe-CNT/GDE	EF	–	250 mL reaction compartment, 11.4 cm^2 graphite anode, 0.05 mol L^{-1} [Na_2SO_4] (electrolyte), pH 3.0, 400 mL min^{-1} O_2 flow rate, 0.1 mmol L^{-1} [Fe^{2+}], −0.85 V voltage	3.23 mmol L^{-1} [H_2O_2] after 90 min electrolysis and 58% current efficiency	[48]
N-doped carbon nanotubes (NCNT)/nickel foam (NF)/CNT	EF	*p*-Nitrophenol	200 mL reaction compartment, 2.25 cm^2 Pt anode, 0.05 mol L^{-1} [Na_2SO_4] (electrolyte), pH 3.0, 400 mL min^{-1} air flow rate, 0.4 mmol L^{-1} [Fe^{3+}], 20 mA cm^{-2} current density	99% removal efficiency for 50 mg L^{-1} *p*-nitrophenol and 0.62 mmol L^{-1} [H_2O_2] after 180 min electrolysis	[49]
Polypyrrole@MWCNT/graphite	EF	Basic Blue 41 (BB 41)	100 mL reaction compartment, 10.0 cm^2 Pt anode and cathode, 0.1 mol L^{-1} [Na_2SO_4] (electrolyte), pH 3.0, 300 mL min^{-1} air flow rate, 2.0 mmol L^{-1} [Fe^{3+}], −0.55 V (vs. SCE) voltage	About 94% removal efficiency for 15 mg L^{-1} BB 41, 0.16 mmol L^{-1} [H_2O_2] after 10 min electrolysis	[50]
N-CNTs-PTFE	EF	MO	250 mL reaction compartment, Pt wire anode, 0.05 mol L^{-1} Na_2SO_4 (electrolyte), pH 3.0, 400 mL min^{-1} O_2 flow rate, 0.2 mmol L^{-1} [Fe^{2+}], −0.85 V voltage	100% removal efficiency for 50 mg L^{-1} MO, 4.28 mmol L^{-1} [H_2O_2] after 60 min electrolysis and 62% current efficiency	[51]

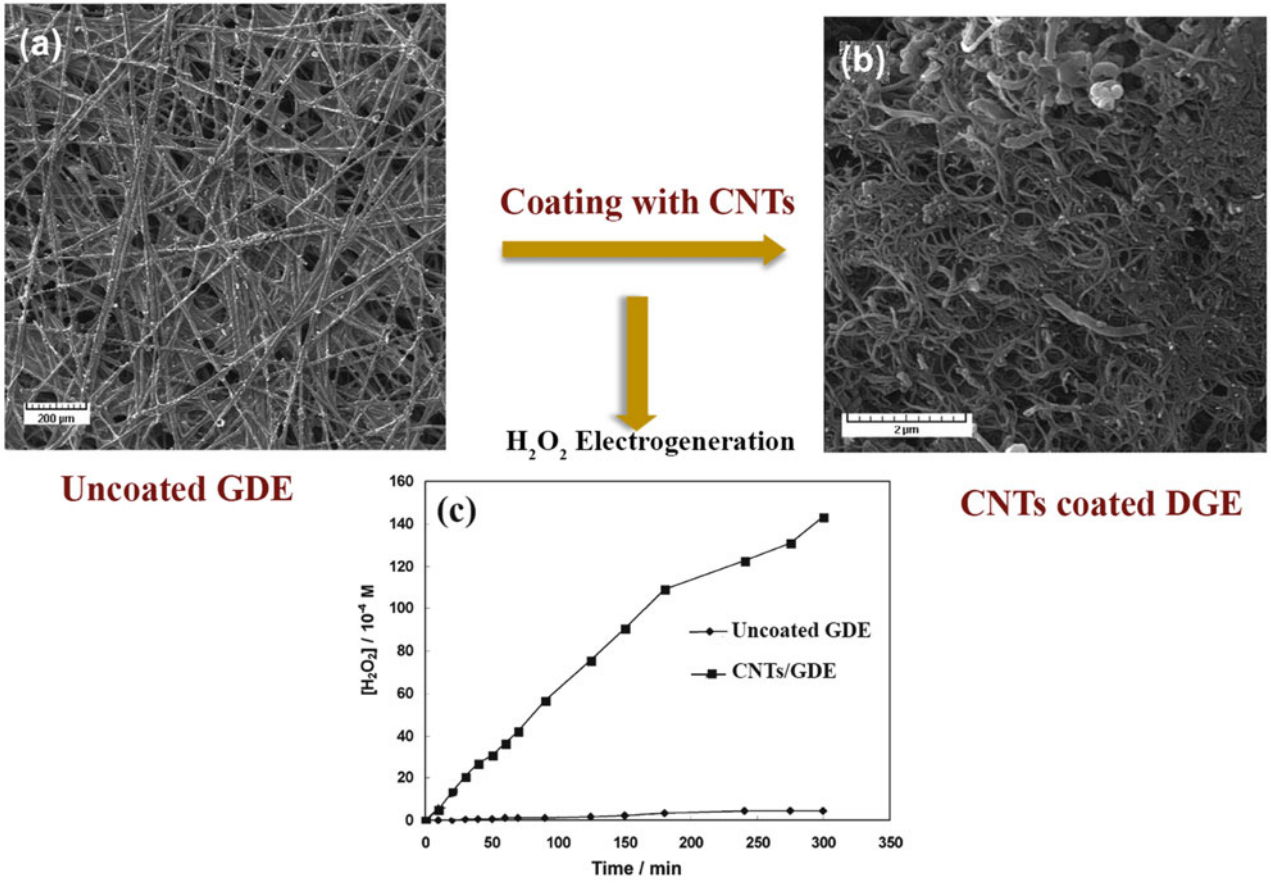

Fig. 4 SEM image of surface of cathodes: (**a**) uncoated GDE, (**b**) CNTs/GDE, and (**c**) the amount of electro-generated H_2O_2 at the uncoated GDE and CNTs/GDE cathodes after 300 min electrolysis (Adapted from [52] with permission from publisher, Elsevier. License Number: 4054120708166)

In another study, graphite electrode was modified by CNTs for treatment of Acid Yellow 36 (AY36) by photo-EF process [5]. The electro-generated H_2O_2 concentration using the CNTs/graphite cathode was approximately seven times greater than that of bare graphite cathode. The decolorization efficiency of AY36 was 31.07 and 70.98% after 120 min of photo-EF treatment for bare graphite and CNTs/graphite, respectively [5]. Also, graphite electrode was modified with MWCNTs accompanied by a cationic surfactant (cetyl trimethyl ammonium bromide (CTAB)) and used as a cathode to degrade two acid dyes by homogeneous and heterogeneous EF processes [46, 47]. The electrodeposition method was used to modify the graphite electrode surface, which was performed by applying the DC voltage to the MWCNTs and CTAB solution. High dye removal efficiency was achieved when MWCNT/graphite was as the cathode compared to the graphite electrode (92% against 64% for 50 mg L^{-1} of dyes), due to the higher electrogeneration of H_2O_2 on the surface of the MWCNT/graphite cathode [46, 47].

Recently, some studies revealed that the introduction of nitrogen atoms to the pristine CNT structure can lead to promote the chemical and electrochemical reactivity of surface for oxygen reduction reaction by the generation of extra electron density in the graphite lattice [33, 38]. Zhang et al. [51] prepared the nitrogen functionalized CNT (N-CNT) electrode as a GDE cathode in EF process. In this study, pulsed high voltage discharge was applied to functionalize MWCNTs in a liquid-gas reactor. The results showed that among three electrodes including graphite, CNTs, and N-CNTs, the N-CNT electrode indicated the highest yield of H_2O_2 formation and faster color removal in EF process. The amount of generated H_2O_2 on the graphite, CNT, and N-CNT electrodes were 2.72, 3.06, and 4.28 mmol L^{-1}, respectively. Furthermore, the N-CNT electrode had the greater current efficiency compared to that of CNT electrode. The results confirmed that the nitrogen functionalization did facilitate the electron transfer to improve the production of H_2O_2.

Nitrogen-doped MWCNTs (N-CNTs) was also used as the catalyst layer on the GDE cathode, which was prepared by immobilizing MWCNTs as the diffusion layer on the surface of nickel foam (NF) as the supporting material [49]. Results showed that the N-CNT/NF/CNT GDE exhibited higher H_2O_2 production amount and greater current efficiency in comparison with the CNT/NF/CNT GDE, consequently, the EF degradation level and total organic carbon (TOC) removal efficiency were higher.

2.2 Graphene Family

Graphene and its derivatives, such as GO, rGO, and few-layer GO, have been thoroughly investigated since their discovery because of their special physical-chemical properties [55]. Graphene, GO, and rGO have different morphological and chemical characteristics as shown in Fig. 5. Pristine graphene consists of a carbon monoatomic layer, 2D planar sheet of carbon atoms in the sp^2 hybridization state, which are densely organized into a honeycomb array (Fig. 5a) [56]. It was first

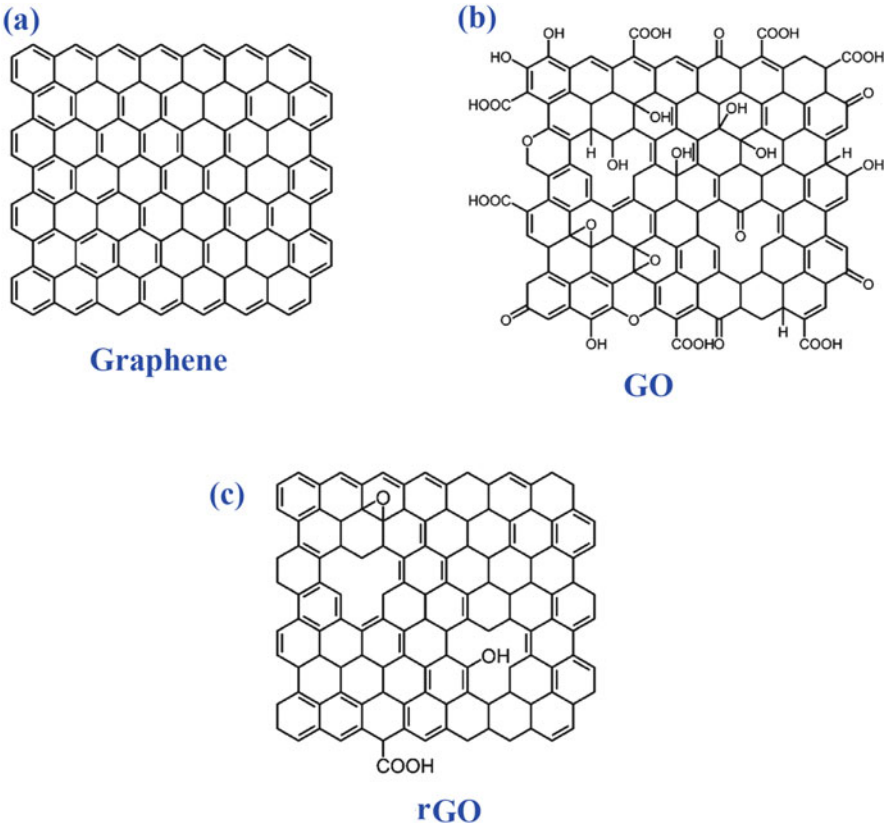

Fig. 5 Schematic illustrating the chemical structure of a single sheet of (**a**) graphene, (**b**) GO, and (**c**) rGO

achieved in 2004 by Novoselov and Geim [57], who prepared graphene sheets by micro-mechanical splitting of oriented pyrolytic graphite and definitively recognized using microscopy. In recognition of the enormous significance of graphene for different applications, its discovery was awarded the 2010 Nobel Prize in Physics. Theoretical and experimental investigations have evidenced that graphene has numerous outstanding properties, comprising a huge specific area (around 2,630 $m^2\ g^{-1}$) [55], exceptional mechanical strength (tensile strength of 130 GPa and Young's modulus of 1,000 GPa) [58], high thermal conductivity (in the range of 4,840–5,300 $W\ m^{-1}\ K^{-1}$) [59], high electrical conductivity (up to 6,000 $S\ cm^{-1}$) [60], great charge-carrier mobility at room temperature ($2 \times 10^5\ cm^2\ V^{-1}\ s^{-1}$) [61], and chemical inertness [62]. Consequently, it is not surprising that graphene has attracted great interest for using in a plethora of various applications, such as supercapacitors, batteries, solar cells, fuel cells, etc. [33, 38].

In general, graphene can be produced either by bottom-up or top-down techniques. The bottom-up method comprises epitaxial growth and chemical vapor

deposition (CVD), including the direct preparation of defect-free graphene from hydrocarbon precursors on solid substrates (Ni or Cu) [38, 63]. Top-down methods, such as electrochemical exfoliation and reduction of GO, refer to the mechanical cleaving of graphite layers for the mass fabrication of graphene sheets. Top-down methodologies present the opportunity to economically synthesize graphene, but it is difficult to obtain high-purity graphene sheets because of the introduction of defects through exfoliation process [29, 38].

The GO is another member of the graphene family, which is an oxygen-functionalized graphene that is fabricated by exfoliation of graphite oxide [64]. The GO is viewed mainly as the precursor to generate graphene [38]. On the GO surface, there are plentiful oxygen-based groups, including epoxy (1,2-ether) (C-O-C) and hydroxyl (−OH) groups, located on the hexagonal array of carbon plane, and carbonyl (−C = O) and carboxyl (−COOH) groups, located at the sheet edges (see Fig. 5b) [56].

The rGO, graphene-like, can be prepared via top-down methods including thermal, chemical, and electrochemical reduction of GO to decrease its oxygen content, with the ratio of C/O rising from 2:1 to up to 246:1 (Fig. 5c) [65]. Although the rGO possesses more defects and thus has less conductivity than pristine graphene, it is enough conductive for use as the electrode material for numerous applications [66]. As graphene, the rGO has also received great attention for different applications in electrochemical devices due to its high specific surface area, functional groups containing oxygen, and hydrophilicity [38]. The oxygen functionalities are opening an adjustable bandgap which is responsible for particular electronic and optical properties [56].

According to the mentioned properties, graphene and its derivatives are alternative candidates for potential use as carbon-based nanomaterials for improving the efficiency of cathode materials employed in EF system. Various scientific reports on applications of graphene family for modification of the cathodes in EF process is summarized in Table 2.

Recently, Mousset and co-workers [76] studied the efficiency of pristine graphene (in the forms of monolayer (G_{mono}), multilayer (G_{multi}), and foam (G_{foam})) as the cathode material in EF process for phenol treatment. It was found that the generated H_2O_2 concentration on the G_{foam} (0.250 mmol L^{-1}) cathode was 5–50 times more than that on the G_{multi} (0.055 mmol L^{-1}) and G_{mono} (0.005 mmol L^{-1}), respectively. The degradation efficiency of 1 mmol L^{-1} phenol was 10.1%, 20.1%, and 62.7% for G_{mono}, G_{multi}, and G_{foam} electrodes, respectively. Therefore, the higher performance of G_{foam} cathode was attributed to its greater electroactive surface area and its higher electrical conductivity than other forms of pristine graphene. Therefore, G_{foam} cathode showed higher phenol degradation and mineralization efficiency than other graphene-based cathodes due to greater rates of $^{\bullet}OH$ formation over Fenton's reaction. Furthermore, less energy consumption and higher mineralization efficiency were achieved by using G_{foam} cathode in comparison with carbon felt cathode, because of the higher electrical conductivity of G_{foam}. The G_{foam} cathode displayed excellent stability as degradation occurred after 10 EF runs.

Table 2 Results reported for modified cathodes with graphene family in EF process

Modified cathode	Process	Pollutant	Operational parameters	Maximum efficiency reported	Ref.
Graphene/graphite-PTFE	EF	Reactive brilliant blue (KN-R)	200 mL three-electrode undivided cell, 6.0 cm^2 Pt sheet counter, SCE reference, 0.05 mol L^{-1} Na_2SO_4 (electrolyte), pH 3, 333 mL min^{-1} O_2 flow rate, 0.75 mmol L^{-1} [Fe^{2+}], 2.0 mA cm^{-2} current density	33.3% TOC decay for 50 mg L^{-1} KN-R, 5.5 mmol L^{-1} [H_2O_2] after 180 min reaction time. 40% current efficiency (for graphite, G, and PTFE solution with the mass ratio of 8:1:2)	[67]
Graphene/glassy carbon	EF	MB	100 mL three-electrode undivided cell, Pt foil counter, SCE reference, 0.1 mol L^{-1} [Na_2SO_4] (electrolyte), pH 3, 11.2 mmol L^{-1} [Fe^{2+}], −1.0 V voltage	97% removal efficiency for 12 mg L^{-1} MB after 160 min reaction time	[36]
ErGO/carbon felt	EF	AO7	30 mL reaction compartment, 2 cm^2 Pt anode, 2 cm^2 cathode surface, 0.05 mol L^{-1} [Na_2SO_4] (electrolyte), pH 3, 0.2 mmol L^{-1} [Fe^{2+}], 20 mA cm^{-2} current density	100% removal efficiency for 100 mg L^{-1} AO7 and 94.3% TOC removal after 20 min EF process	[68, 69]
Graphene-PPy/polyester filter cloth/fabric membrane	EF-cathodic membrane filtration	MB	50 mL reaction compartment, stainless iron mesh anode, 0.05 mol L^{-1} [Na_2SO_4] (electrolyte), pH 4, 200 mL min^{-1} air flow rate, 0.2 mmol L^{-1} [Fe^{2+}], −1.0 V voltage, 99 L m^{-2} membrane flux	95% removal efficiency for 5 mg L^{-1} MB in 90 min	[70]
ErGO/GDE	Cathodic electrochemical advance oxidation	BPA	30 mL electrochemical reactor, 1.0 cm^2 Pt anode, 0.05 mol L^{-1} [Na_2SO_4] (electrolyte), pH 6.5, 2.86 mA cm^{-2} current density, 60 min electrolysis for rGO	100% removal efficiency for 20 mg L^{-1} BPA and 74.6% TOC removal in 30 min and 1.17 mmol L^{-1} [H_2O_2] in 60 min electrolysis time	[71]
Graphene @Fe_3O_4/Ni foam	Heterogeneous-EF	MB	150 mL reaction compartment, 8.0 cm^2 Pt anode, 0.05 mol L^{-1} [Na_2SO_4] (electrolyte), pH 2.0, 0.5 mA cm^{-2} current density	97% removal efficiency for 10 mg L^{-1} MB in 24 min	[72]

(continued)

Table 2 (continued)

Modified cathode	Process	Pollutant	Operational parameters	Maximum efficiency reported	Ref.
Graphene@PTFE	EF	2,4-Dichlorophenol (2,4-DCP) and Rh B	50 mL reaction compartment, 1.0 cm^2 Pt anode, 0.07 mol L^{-1} [Na_2SO_4] (electrolyte), pH 3.0, 2.0 mmol L^{-1} [Fe^{2+}], 40 mA cm^{-2} current density	100% and 97.6% removal efficiency for Rh B and 2,4-DCP, respectively, 0.17 mmol L^{-1} [H_2O_2] in 150 min electrolysis and 58% current efficiency	[73]
Pd@rGO/carbon felt	EF	EDTA-Ni	450 mL reaction compartment, 54 cm^2 graphite tube anode, 35 cm^2 cathode surface/ 0.05 mol L^{-1} [Na_2SO_4] (electrolyte), pH 4.0, 1.0 mmol L^{-1} [Fe^{2+}], 5.7 mA cm^{-2} current density	83.8% removal efficiency for 10 mg L^{-1} EDTA-Ni in 100 min treatment	[74]
AQ@ErGO/Ni screen	Heterogeneous-EF	Rh B	200 mL reaction compartment, Pt wire anode, 0.5 mol L^{-1} [Na_2SO_4] and [$MgSO_4$] (electrolyte), pH 3.4 and 11.3, 600 mL min^{-1} O_2 flow rate, 100 g L^{-1} FeOOH-γ-Al_2O_3, −0.5 V voltage	100% removal efficiency for 10 mg L^{-1} Rh B,4.83 mmol L^{-1} [H_2O_2] in 120 min reaction time and 83.4% and 67.5% current efficiency for Na_2SO_4 and $MgSO_4$ as electrolytes, respectively	[75]
3D graphene foam	EF	Phenol	150 mL reaction compartment, 30 cm^2 Pt anode, 20 cm^2 cathode surface area, 0.05 mol L^{-1} [K_2SO_4] (electrolyte), pH 3.0, 200 mL min^{-1} air flow rate, 0.1 mmol L^{-1} [Fe^{2+}], −0.6 V voltage	78% removal efficiency for 1.0 mmol L^{-1} phenol and 0.25 mmol L^{-1} [H_2O_2] in 120 min electrolysis	[76]
Graphene/carbon cloth			80 mL reaction compartment, 15 cm^2 Pt anode, 24 cm^2 cathode surface area, 0.05 mol L^{-1} [K_2SO_4] (electrolyte), pH 3.0, 200 mL min^{-1} air flow rate, 0.1 mmol L^{-1} [Fe^{2+}], 1.25 mA cm^{-2} current density	80% removal efficiency for 1.4 mmol L^{-1} phenol and 40% TOC removal and 2.00 mmol L^{-1} [H_2O_2] in 120 min electrolysis	[34]
N-doped graphene@MWC-NT/stainless steel	EF	Dimethyl phthalate (DMP)	100 mL reaction compartment, 4 cm^2 Pt foil anode, 0.05 mol L^{-1} [Na_2SO_4] (electrolyte), pH 3.0, 450 mL min^{-1} air flow rate, 0.5 mmol L^{-1} [Fe^{2+}], −0.2 V voltage	99% removal efficiency for 50 mg L^{-1} DMP and 9.03 mmol L^{-1} [H_2O_2] after 120 min electrolysis	[77]

CeO_2/rGO	EF	Ciprofloxacin (CIP)	250 mL reaction compartment, 0.5 cm^2 Pt anode, 24 cm^2 cathode surface area, 0.05 mol L^{-1} [Na_2SO_4] (electrolyte), pH 3.0, 100 mL min^{-1} O_2 flow rate, 0.1 mmol L^{-1} [Fe^{2+}], 53.3 mA cm^{-2} current density	90.97% removal efficiency for 50 mg L^{-1} CIP in 6.5 h treatment	[78]
$Ce_{0.75}Zr_{0.25}O_2$/rGO				100% removal efficiency for 50 mg L^{-1} CIP in 5 h treatment	[79]
Quinone@graphene@Fe_3O_4/carbon cloth	Heterogeneous-EF	BPA	60 mL undivided cylindrical cell, 10.0 cm^2 Pt anode, 10.0 cm^2 cathode surface area, Ag/AgCl reference electrode, 0.05 mol L^{-1} [Na_2SO_4] (electrolyte), pH 3.0, 1000 mL min^{-1} air flow rate, −2.4 V voltage	100% removal efficiency for 5 mg L^{-1} BPA in 90 min treatment and 4.37 mmol L^{-1} [H_2O_2] at pH 3	[80]

In another study by this group [34], high purity of graphene was prepared by electrochemical exfoliation. Synthesized graphene was combined with Nafion as a binder to make a conductive ink which was then employed to modify the carbon cloth electrode [34]. The optimal amounts of graphene and Nafion in the ink were found to be 1.0 mg mL^{-1} and 0.025% (w/v), respectively, with a graphene mass loading of 0.27 mg cm^{-2} on the carbon cloth surface. A graphical illustration of preparation of graphene-modified carbon cloth electrode is depicted in Fig. 6. The results showed that the graphene-modified carbon cloth cathode improves electrochemical properties, such as the 97% decline of the charge transfer resistance and an 11.5-fold increment of the electroactive surface area compared with raw carbon cloth [34]. As illustrated in Fig. 6, the maximum electro-generated H_2O_2 concentrations were 1.01 mmol L^{-1} and 1.99 mmol L^{-1} for the uncoated and graphene-coated carbon cloth cathodes, respectively [34]. The superior electrochemical behaviors of the graphene-coated carbon cloth cathode were further proved by the improved performance in EF process for degradation of phenol. Thus, the pseudo-first-order kinetic rate constant (k_{app}) values of phenol degradation on the uncoated and graphene-coated carbon cloth cathodes were 0.0051 and 0.0157 min^{-1}, respectively, a 3.08-fold increase.

Le et al. [68, 69] modified CF electrode with rGO, which was prepared by an electrophoretic deposition of GO and was reduced with the different methods including electrochemical, chemical, and thermal. Among the used reduction methods, the electrochemical reduction of GO under a constant potential (−0.45 V vs. SCE) without addition of any binder or reductant demonstrated remarkable advantages. The schematic of preparation of electrochemically reduced GO (ErGO)/CF electrode and SEM images of ERGO/CF and raw CF were presented in Fig. 7. The ErGO/CF cathode demonstrated significant electrochemical behaviors, such as the enhancement of electroactive surface area and the decline in charge transfer resistance compared to the raw CF cathode. This improvement accelerated the O_2 reduction rate on the cathode surface, which significantly increased the H_2O_2 accumulation in the solution. Consequently, the destruction rate of Acid Orange 7 (AO7) by the EF process was two times greater on the ErGO/CF cathode compared to uncoated CF. TOC removal after 2 h degradation was 73.9% on the ErGO/CF electrode, and this was 18.3% greater than on the unmodified CF (Fig. 7c). Moreover, the ErGO/CF cathode presented good stability over ten runs of EF process for mineralization of AO7.

Chen et al. [36] modified the glassy carbon electrode and studied the effect of annealing temperature of GO (250 and 1,000°C) on the electro-generated H_2O_2 efficiency in EF process. The results indicated that the thermally reduced GO annealed at 250°C (G250) was more efficient for mineralization of methylene blue (MB) by the EF method. The oxygen functionalities in G250 were responsible for the high two-electron oxygen reduction selectivity and highest formation rate of H_2O_2 [36].

The results of studies obviously indicated that modification of carbon-based electrode surface with quinone functional groups could remarkably improve the redox activity of the electrode and facilitate the two-electron reduction of O_2 to H_2O_2 reaction on the cathode [75, 80–82]. Zhang and co-worker [75] studied the

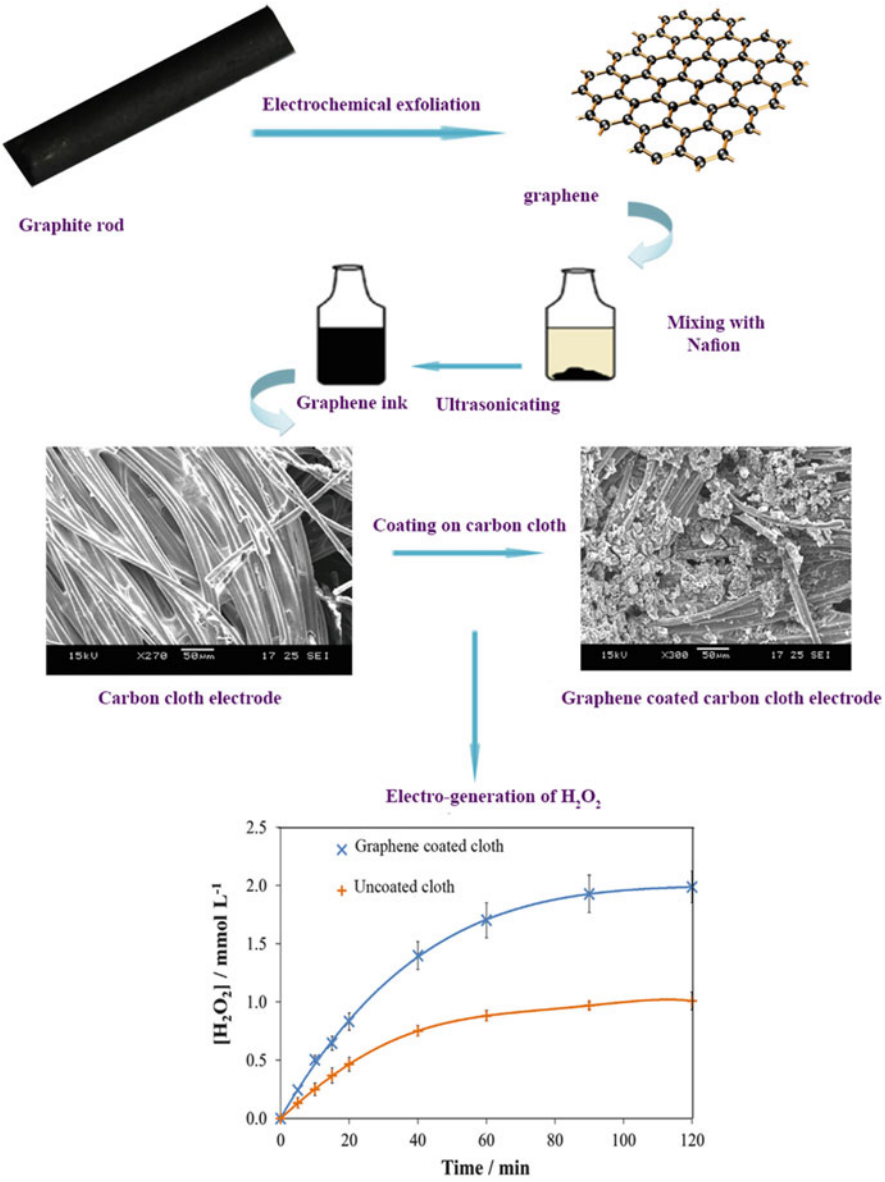

Fig. 6 Schematic steps of preparation of graphene-coated carbon cloth cathode and H_2O_2 accumulation yield of uncoated and graphene-coated carbon cloth cathodes (SEM images and H_2O_2 accumulation yield curves adapted from [34], with permission from Elsevier. License Number: 4047601289247)

electro-generation of H_2O_2 on anthraquinone@ErGO (AQ@ErGO) coated on nickel screen surface cathode and its performance for degradation of Rh B by FeOOH-catalyzed heterogeneous EF process. The strong interfacial connections of

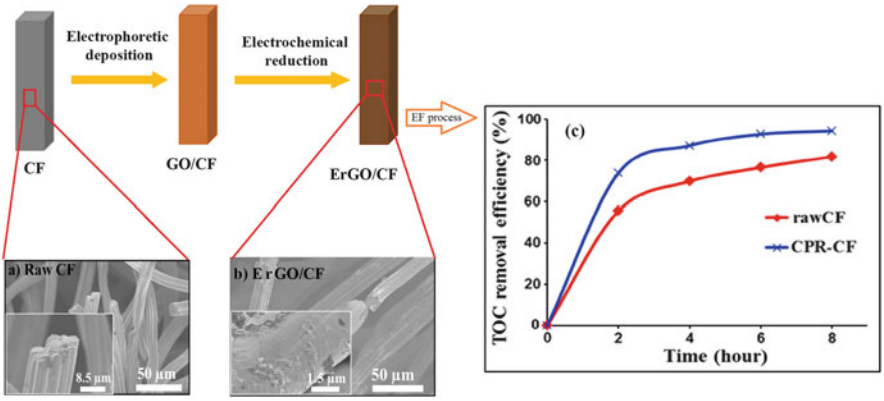

Fig. 7 Schematic steps of preparation of ErGO/CF cathode, SEM images of (**a**) raw CF, (**b**) ErGO/CF, and (**c**) TOC removal after 8 h EF process using raw CF and ErGO/CF cathodes. (Adapted from [68], with permission from Elsevier. License Number: 4036640134966)

ErGO and AQ molecules led to the efficient production of H_2O_2 at the cathode. The AQ@ErGO cathode can efficiently catalyze the two-electron reduction of O_2 to produce H_2O_2 (reactions (5) and (6)) on the cathode/bulk solution interface:

$$\equiv AQ + 2H^+ + 2e^- \rightarrow \equiv H_2AQ \quad (5)$$

$$\equiv H_2AQ + O_2 \rightarrow \equiv AQ + H_2O_2 \quad (6)$$

The accumulated concentration of H_2O_2 was obtained at 4.01 and 4.86 mmol L^{-1} in 0.5 mol L^{-1} $MgSO_4$ and Na_2SO_4 electrolyte, respectively, after 120 min of electrolysis. Then, electro-generated H_2O_2 molecules are catalytically converted into $^{\bullet}OH$ by the FeOOH nanoparticles, and the dissolved iron ions in $MgSO_4$ catholyte. Since, no dissolved iron ions were detected in Na_2SO_4 catholyte, the high yield of the hetero-EF process is ascribed generally to the H_2O_2 activation through the surface of FeOOH nanoparticles to form $^{\bullet}OH$ and $HO_2^{\bullet}$ ($O_2^{\bullet -}$).

Zhao et al. [70] synthesized the graphene/polypyrrole (PPy) modified conductive cathode membrane for the EF filtration treatment of MB as a model pollutant. The better performance of membrane cathode for treatment of MB was obtained by doping with anthraquinone monosulfonate (AQS). The observed performance enhancement can be attributed to the electrical conductivity improvement, resulted by doping with AQS [70].

In recent years, researchers studied the several carbon nanocomposites with metal/metal oxide for modification of electrodes in EF process. Magnetite (Fe_3O_4) seems to be promising candidate for this purpose owing to its reversible redox nature and stability. These modified electrodes revealed extraordinary mechanical stability, making them noteworthy as stable materials for in situ generation of H_2O_2 and $^{\bullet}OH$, diminishing the iron sludge formation, exhibiting much higher activity than homogenous EF systems under a neutral pH.

Shen et al. [72] synthesized graphene-Fe_3O_4 (G-FeO) hollow hybrid microspheres by a simple aerosolized spray drying method by using ferric ion and GO with various contents (e.g., 0, 5, 15, 30 wt%) as the precursor materials. Subsequently, the obtained composites were coated on the surface of Ni foam cathode. The results of electrochemical studies obviously indicated that the G-FeO composite with graphene content of 30 wt% (30G–FeO) exhibited higher conductivity and lower charge transfer resistance. Also, the two-electron pathway was the dominated process for O_2 reduction on the 30G–FeO electrode. The yield of H_2O_2 generation notably increased when 30G–FeO was applied as the cathode in EF process. The MB degradation rate constant value of 30G–FeO coated Ni foam cathode at pH 2 was 0.140 min^{-1}, which was nearly 8.75 times greater than that for the uncoated Ni foam cathode (0.016 min^{-1}). Figure 8 shows the schematic illustration of EF system and mechanism for MB degradation process on the 30G–FeO cathode.

Researches revealed that palladium (Pd) nanoparticles could interact with graphene-based materials and exhibited extraordinary electrocatalytic ability. Zhang et al. [74] modified CF cathode with Pd@rGO composite and Nafion as a binder. Pd@rGO/CF cathode exhibited high electrocatalytic activity and stability for the elimination of ethylenediaminetetraacetic acid (EDTA)-Ni complex solution by the EF method.

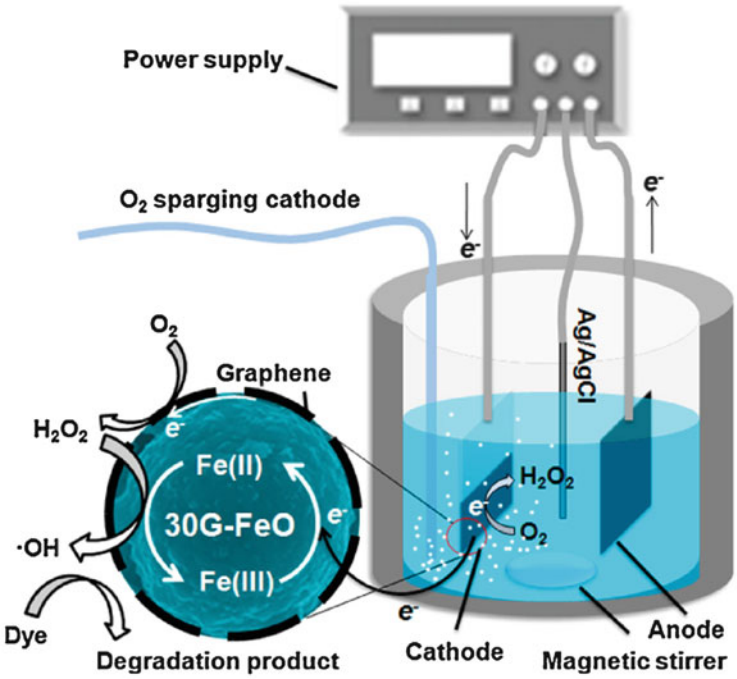

Fig. 8 Schematic illustration of EF system and mechanism for MB degradation process on the 30G–FeO cathode (Reprinted from [72], with permission from Elsevier. License Number: 4037580393197)

Govindaraj et al. [80] synthesized a quinone-functionalized graphene by the electrochemical exfoliation approach (QEEG) followed by prepared QEEG@Fe_3O_4 nanocomposite. Then, QEEG and prepared nanocomposite were used for modifying the surface of the noncatalyzed carbon cloth (NCC) electrode. The SEM images of the NCC and the modified NCC are shown in Fig. 9a. The obtained results demonstrated that the produced H_2O_2 concentration at the QEEG electrode was approximately nine times higher than that at the NCC electrode at pH 3.0 and four times greater at natural pH (see Fig. 9b), which can be attributed to the presence of the quinone functional group and high electroactive surface area in the QEEG structure. Substantial improvement in the electro-generation of $^{\bullet}OH$ radicals was observed with QEEG@Fe_3O_4 modified cathodes. Complete degradation of Bisphenol A (BPA) by EF process was achieved using the QEEG@Fe_3O_4 modified electrode in 90 min at pH 3. Also, 98% degradation yield was obtained at neutral condition with less than 1% of iron leaching. Schematic illustration of the overall mechanisms relating to QEEG@Fe_3O_4 modified cathode in the EF treatment of BPA is shown in Fig. 9c.

2.3 Mesoporous Carbons

In the past two decades, mesoporous carbons (with pore size distribution in the range 2–50 nm) have attracted great consideration for use as electrode materials in various applications [29]. These carbon-based nanomaterials have delivered noteworthy advantages such as high specific surface areas for a huge number of surface-active sites, good electrical conductivity for facile electron transport, large accessible space for fast mass transport, high mechanical and chemical durability for powerful electrode longevity, and low density [83]. The synthetic approaches comprising hard and soft templates have established to be the most effective methods for the construction of mesoporous carbons with distinct pore structures and narrow distribution of pore sizes [29]. In these preparation methods, mesoporous carbon structures can be obtained after curing of carbonaceous precursor, elimination of template, and carbonization. In the hard templating method, inorganic templates (hard templates), including metal-organic frameworks (MOFs), zeolites, silicas, and MgO, were employed to synthesize ordered mesoporous carbons (OMC) [29, 83]. Silica templates with ordered mesoporous framework were prepared by templating self-formation of surfactants, such as SBA-15, MCM-48, and MCM-41 [83]. Schematic graphic of the preparation of OMC by silica hard templates is shown in Fig. 10. On the other hand, in the soft templating technique, phenolic resin and some block copolymer surfactants were mainly used as organic templates to produce highly OMC through organic-organic assembly of surfactants and phenolic resins [29]. Additionally, by incorporating soft and hard templating approaches, hierarchically porous carbon (HPC), sometimes described as carbon nanoarchitecture, with organized porosity on multiple levels can be achieved [29, 84].

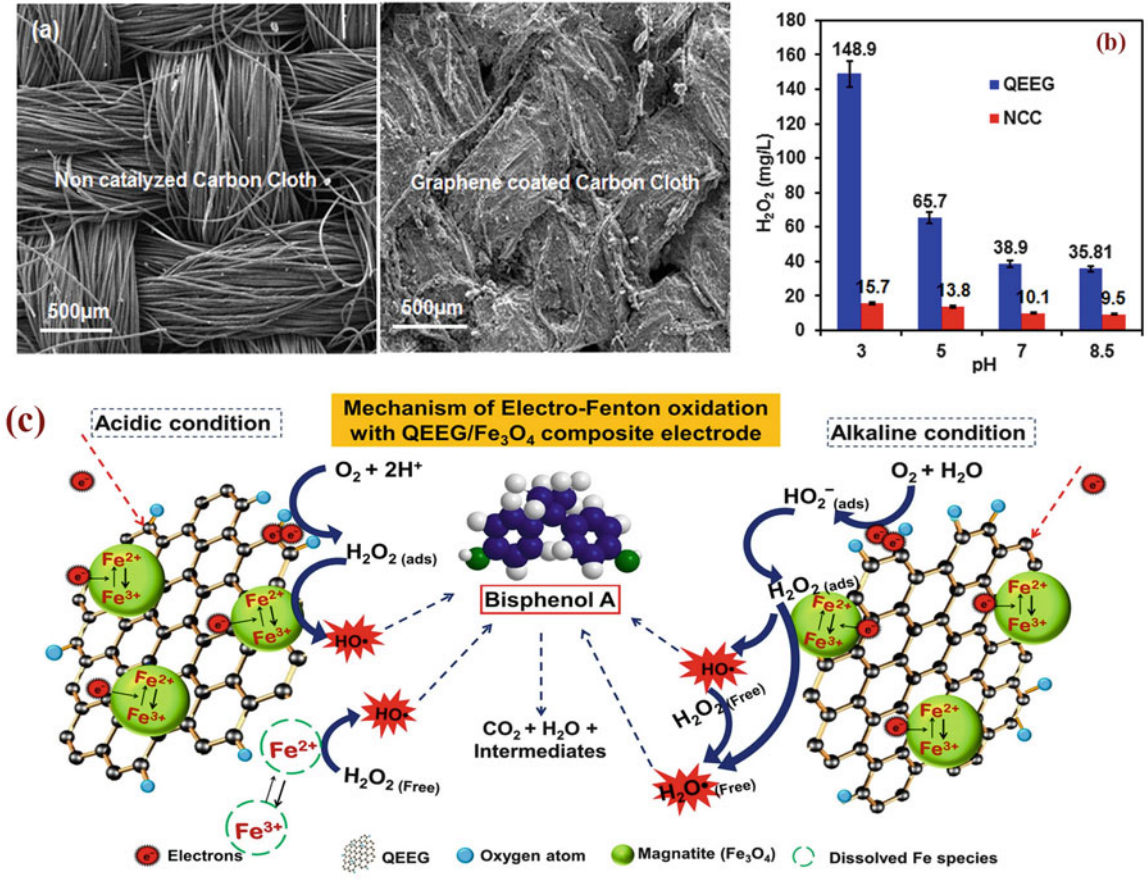

Fig. 9 (**a**) SEM images of NCC and QEEG coated carbon cloth, (**b**) difference in H_2O_2 formation with NCC and QEEG modified cathodes, and (**c**) schematic illustration of the overall mechanisms relating to QEEG/Fe_3O_4 modified cathode in the EF treatment of BPA (Reprinted from [80], with permission from Elsevier. License Number: 4047001318719)

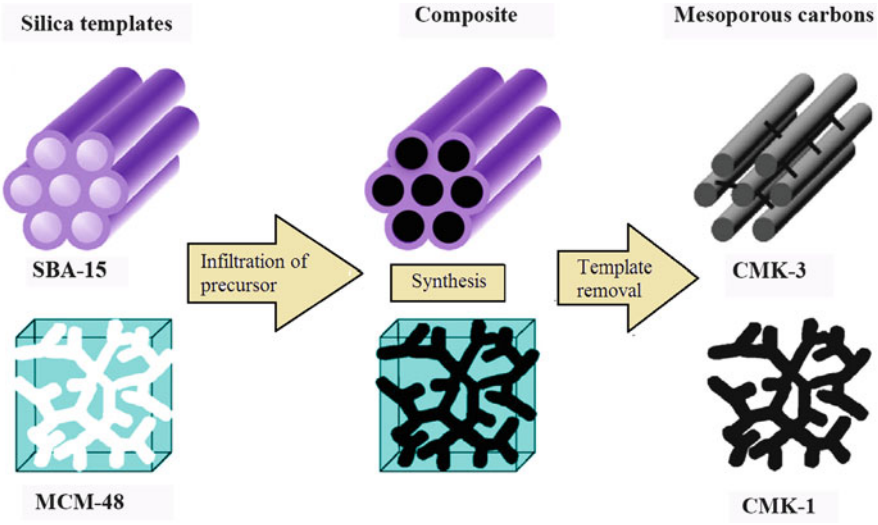

Fig. 10 Schematic graphic of the preparation of OMC by silica hard templates

Recently, mesoporous carbons have been considered to be exceptional candidates for modification of cathode electrode in EF process, which can facilitate the diffusion and transformation of O_2 at the cathode surface and enhance the electrogeneration yield of H_2O_2 [85–88]. Table 3 summarizes the main reported modified cathode with CNTs and their derivatives in EF process. Hu et al. [85] grafted the surface of activated carbon fiber (ACF) cathode with OMC, which was prepared by soft templating method. For comparison, ACF was also modified with a layer of disordered mesoporous carbon (DMC). The results demonstrated that the production rate of $^{\bullet}OH$ radicals pursued the order of OMC/ACF > DMC/ACF > ACF, which was in accordance with the H_2O_2 generation rate and Brilliant Red X3B (X3B) degradation rate. A graphical illustration of preparation of OMC modified ACF cathode is depicted in Fig. 11.

As previously mentioned, heteroatom (e.g., sulfur and nitrogen) doping of carbon materials can improve their surface attributes, specifically the electrical conductivity and the polarity of surface. For this aim, nitrogen-doped mesoporous carbons were prepared by nitrogenous precursors. For instance, nitrogen-doped OMC (N-OMC) was prepared by dicyandiamide ($C_2H_4N_4$) and was coated onto the surface of ACF cathode (N-OMC/ACF), which showed more electrocatalytic activity and lower overpotential for O_2 reduction compared to OMC/ACF cathode in the EF process [86].

Perazzolo et al. [91, 92] synthesized nitrogen- and sulfur-doped or co-doped mesoporous carbons (N-MC, S-MC, and N,S-MC) by means of a hard template method and used them for modifying glassy carbon electrode for the in situ formation of H_2O_2 and degradation of MO by the EF system. The N-MC modified

Table 3 Results reported for modified cathodes with mesoporous carbons in EF process

Modified cathode	Process	Pollutant	Operational parameters	Carbon mesoporous characteristics	Maximum efficiency reported	Ref.
OMC/ACF	EF	X3B	200 mL reaction compartment, 12 cm^2 Pt, 9.0 cm^2 cathode surface, 0.1 mol L^{-1} [Na_2SO_4] (electrolyte), pH 3.0, 1.0 mmol L^{-1} [Fe^{2+}], 600 mL min^{-1} air flow rate, 6.2 V voltage	S_{BET} = 722 m^2 g^{-1} Mesopore volume = 0.19 cm^3 g^{-1}	The EF degradation rate constant value of X3B in OMC/ACF cathode (0.055 min^{-1}) was larger than in ACF cathode (0.018 min^{-1}). 80.6% of TOC depletion was found within 60 min when using OMC/ACF cathode. The maximum H_2O_2 concentration was of 9.4 μmol L^{-1} and 7.1 μmol L^{-1} in OMC/ACF and ACF cathode, respectively	[85]
N-doped OMC/ACF			250 mL reaction compartment, 9.0 cm^2 graphite anode, 9.0 cm^2 cathode surface, 0.1 mol L^{-1} [Na_2SO_4] (electrolyte), pH 3.0, 1.0 mmol L^{-1} [Fe^{2+}], 600 mL min^{-1} air flow rate, 3.0 V voltage	Mass of dicyandiamide = 1.0 g S_{BET} = 501 m^2 g^{-1} Pore volume = 0.35 cm^3 g^{-1} Mean pore size = 3.5 nm	The degradation rate of X3B by using of N (1.0)-OMC/ACF cathode was 50% higher than that of the OMC/ACF cathode. The maximum H_2O_2 concentration was of 40.93 μmol L^{-1} and 21.75 μmol L^{-1} in N(1.0)-OMC/ACF and OMC/ACF cathode, respectively	[86]
OMC-5.4/ACF	EF	Rh B	200 mL reaction compartment, 12 cm^2 Pt anode, 9.0 cm^2 cathode surface, 0.1 mol L^{-1} [Na_2SO_4] (electrolyte), pH 3.0, 1.0 mmol L^{-1} [Fe^{2+}], 600 mL min^{-1} air flow rate, −0.1 V voltage	S_{BET} = 486 m^2 g^{-1} Pore volume = 0.45 cm^3 g^{-1} Mean pore size = 5.4 nm	100% of Rh B was degraded by OMC-5.4/ACF within 45 min, whereas the degradation rate of Rh B in the presence of OMC-3.7/ACF and OMC-2.6/ACF decreased to 93.2% and 71.2%, respectively. The concentration of	[87]

(continued)

Table 3 (continued)

Modified cathode	Process	Pollutant	Operational parameters	Carbon mesoporous characteristics	Maximum efficiency reported	Ref.
					H_2O_2 was 2.02 mmol L^{-1} in OMC-5.4/ACF, while it was 1.79 mmol L^{-1} in OMC-3.7/ACF as cathode materials	
rGO@OMC/ACF	EF	Dimethyl phthalate (DMP)	200 mL reaction compartment, 12 cm^2 Pt anode, 9.0 cm^2 cathode surface, 0.1 mol L^{-1} [Na_2SO_4] (electrolyte), pH 3.0, 1.0 mmol L^{-1} [Fe^{2+}], 600 mL min^{-1} air flow rate, −0.7 V voltage	Dosage of rGO = 30 mg S_{BET} = 533.3 m^2 g^{-1} Mean pore size = 3.8 nm	The concentration of H_2O_2 increased with the dosage of rGO from 0 to 30 mg, but considerably diminished from 30 to 90 mg. The maximum H_2O_2 concentration was of 2.5 mmol L^{-1} with the current efficiency of 40.4%. rGO30@OMC/ACF indicated the highest DMP removal efficiency with an apparent rate constant value of 0.049 min^{-1}, about 1.5 times to that at OMC/ACF	[35]
CMK-3/GDE	EF	DMP	200 mL three-electrode undivided cell, Pt foil counter, SCE reference, 4.0 cm^2 cathode surface, 0.1 mol L^{-1} [Na_2SO_4] (electrolyte), pH 3.0, 300 mL min^{-1} O_2 flow rate, 0.5 mmol L^{-1} [Fe^{2+}], −0.5 V voltage	S_{BET} = 992 m^2 g^{-1} Pore volume = 0.45 cm^3 g^{-1} Mean pore size = 4.3 nm	The accumulative H_2O_2 concentrations obtained at the CMK-3/GDE, graphite GDE, and carbon paper were increased to 1.29, 0.41, and 0.29 mmol L^{-1}, respectively. The apparent rate constant values of DMP degradation at the CMK-3/GDE, graphite GDE, and carbon paper cathode were 0.300, 0.034, and 0.026 min^{-1}, respectively	[89]

Fe-GMCA[a]/Ni foam	Heterogeneous-EF	MB	100 mL three-electrode undivided cell, 8.0 cm^2 Pt sheet counter, Ag/AgCl reference, 8.0 cm^2 cathode surface, 0.05 mol L^{-1} [Na_2SO_4] (electrolyte), pH 3.0, 400 mL min^{-1} O_2 flow rate, 15 mA applied current	S_{BET} = 479.8 m^2 g^{-1} Pore volume = 0.74 cm^3 g^{-1} Mean pore size = 3.1 nm	The concentrations of generated H_2O_2 at the GMCA/Ni foam and Ni foam cathodes were 1.26 and 0.51 mmol L^{-1}, respectively. The degradation rate constant values of MB were 0.072 min^{-1}, 0.043 min^{-1}, and 0.030 min^{-1} for Fe-GMCA, Fe-GCA, and Fe-MCA, respectively	[90]
N, S-doped MC/glassy carbon	Electrochemical oxidation	Methyl orange (MO)	100 mL three-electrode undivided cell, graphite rod counter, SCE reference, 6.0 cm^2 cathode surface, 0.05 mol L^{-1} [Na_2SO_4] (electrolyte), pH 2.4, 400 mL min^{-1} O_2 flow rate, −0.5 V vs. SCE voltage	S_{BET} (N-doped MC) = 881 m^2 g^{-1} Mean pore size (N-doped MC) = 3.7 nm S_{BET} (S-doped MC) = 1,103 m^2 g^{-1} Mean pore size (S-doped MC) = 3.7 nm S_{BET} (N, S-doped MC) = 855 m^2 g^{-1} Mean pore size (N,S-doped MC) = 3.7 nm	Degradation efficiencies of MO were around 100%, 70%, and 60% when N-MC, S-MC, and N,S-MC were applied as electrode material, respectively	[91, 92]
HPC/carbon paper	EF	Perfluorooctanoate (PFOA)	60 mL three-electrode undivided cell, 6.0 cm^2 Pt sheet counter, SCE reference, 10 cm^2 cathode surface, 0.05 mol L^{-1} [Na_2SO_4] (electrolyte), pH 2.0, 1.0 mmol L^{-1} [Fe^{2+}], −0.4 V vs. SCE voltage	Hydrothermal time: 24 h S_{BET} = 2,130 m^2 g^{-1} Pore size distribution: 1.0–10.0 nm	The electro-generated H_2O_2 concentration on the modified cathode with HPC was 142.5 mmol L^{-1} with current efficiency of 91.2%. PFOA was degraded with removal efficiency of 94.3% in 120 min	[88, 93]

[a]Iron oxide containing graphene/carbon nanotube based carbon aerogel

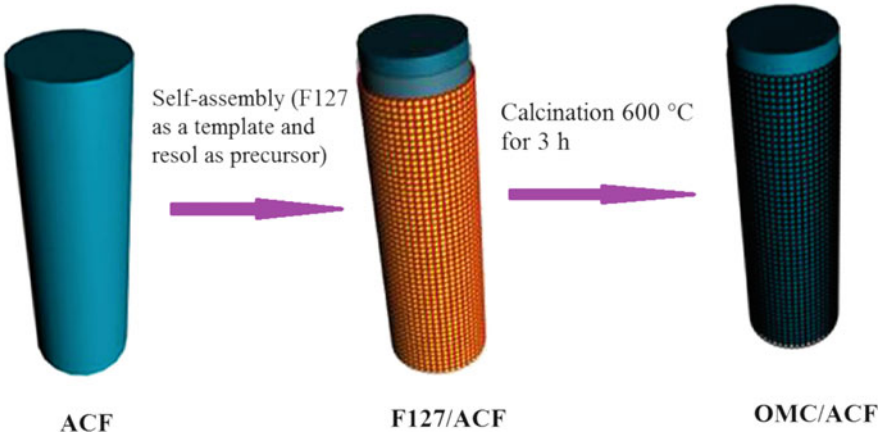

Fig. 11 A graphical illustration of preparation of OMC modified ACF cathode

electrode showed higher performance in EF process compared with S-MC and N, S-MC modified electrodes.

The correlation between mesoporous structure and efficiency of cathode materials in the EF method was investigated [87]. In this research, OMCs with average pore size of 2.6, 3.6, and 5.4 nm were prepared by means of boric acid as the expanding agent and coated on the surface of ACF. Figure 12a, b show TEM images of OMC-3.7/ACF and OMC-5.4/ACF. H_2O_2 accumulation and degradation profiles of Rh B in EF system in the as-prepared cathodes is illustrated in Fig. 12c, d, respectively. It was found that the large pore size (5.4 nm) promotes the mass transfer of O_2 on the surface of the modified cathode, which then results in high generation of H_2O_2 and consequently enhances the degradation efficiency. After ten consecutive EF runs, the reactivity of OMC-5.4/ACF cathode remained approximately unchanged.

In another research, rGO was employed to fabricate rGO@OMC/ACF cathode with lower impedance and better electroactive surface area compared with OMC/ACF, which improved the H_2O_2 production and current efficiency of the EF process. The observed electrochemical performance enhancement can be attributed to the electrical conductivity improvement, resulted by coating of rGO.

Wang and co-workers [89] synthesized CMK-3-type OMC with a pore size of around 4.3 nm by applying the SBA-15 as a hard template. Then, carbon paper was covered by as-prepared CMK-3 to fabricate the GDE cathode with high porosity and large surface area. Using this electrode, the side reaction of H_2 evolution is minimized at a low cathodic potential; thus the H_2O_2 formation is increased to rapidly degrade organic pollutant such as dimethyl phthalate (DMP) by EF process.

Recently, Liu et al. [88, 93] coated the carbon paper surface with HPC which was prepared by hydrothermal synthesis of MOF-5 as a hard template, and then its carbonization resulted HPC to exhibit high amount of sp^3 carbon hybridization and defects, huge surface area (2,130 $m^2\ g^{-1}$), and rapid O_2 mass transport. The modified carbon paper presented a high selectivity for the O_2 reduction to H_2O_2

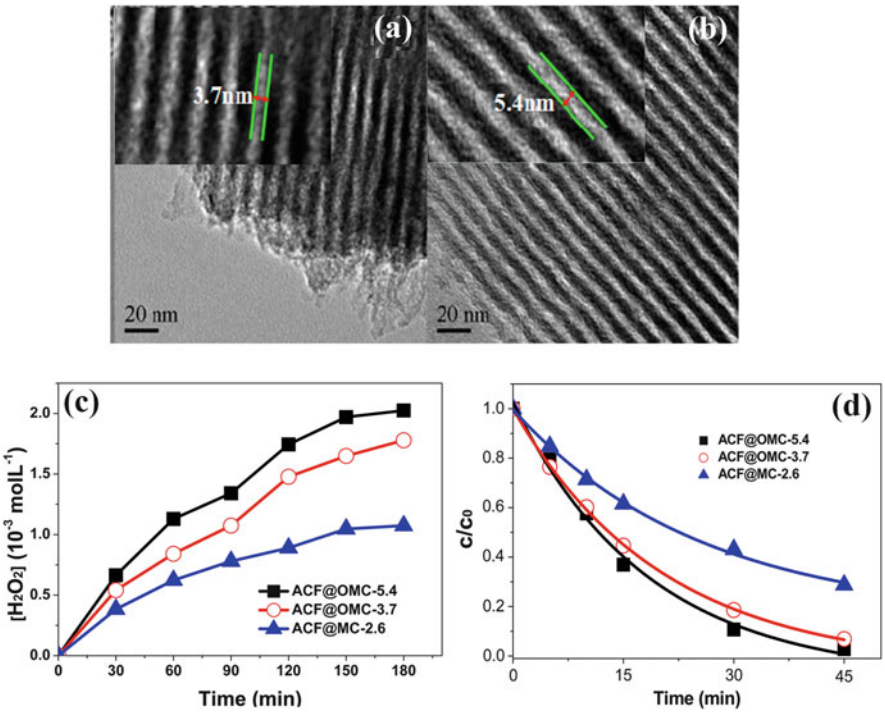

Fig. 12 TEM images of (**a**) OMC-3.7/ACF, (**b**) OMC-5.4/ACF, (**c**) H_2O_2 accumulation, and (**d**) degradation profiles of Rh B in EF system in the as-prepared cathodes (Reprinted with the permission from [87], Copyright 2015 American Chemical Society)

in a broad range of pH (1–7). Perfluorooctanoate (PFOA) was efficiently treated by using HPC modified cathode at low potential (−0.4 V). The superior efficiency of this EF process can be ascribed to high H_2O_2 generation at the modified cathode at low energy consumption, demonstrating their promising application for efficient treatment of recalcitrant pollutants in wastewater.

3 Conclusion

The main concern with the EF process is to improve the generation of H_2O_2 and enhance the reduction rate of ferric ions on the cathode for effective destruction of pollutants. Thus, it is worthwhile to further develop the performance of cathode with its surface modification. Recently, carbon-based nanomaterials have attracted substantial attention due to their superior physicochemical properties including high specific surface area, good electronic conductivity, chemical inertness, and facile surface modification capability. This chapter discussed the modified cathodes with carbon-based nanomaterials, e.g., CNTs, graphene family, and mesoporous

carbons, for EF system. Progress in the modification of cathodes with these nanomaterials for performance development of EF process has been tremendous in recent years, opening novel alternatives in the degradation of recalcitrant pollutants in wastewater.

Despite the extensive research on the modification of cathodes in EF processes, several challenges still need to be addressed to optimize the design of these cathodes for industrial applications at a large scale. First, a technique for better coating or condensing of carbon nanomaterials needs to be further explored. Due to the fact that nanomaterials may be leached from the coated bed, the efficient coating approaches should be developed. Second, carbon nanomaterials generally have a strong tendency to agglomerate owing to their nanosize and high surface energy. Therefore, their applications are limited due to the difficulty in dispersing them in a solvent (water or organic agent) for coating on the electrode. Improved dispersion of carbon nanomaterials could be achieved by modifying their surfaces or optimizing the coating process. Also, this matter could be resolved by preparing of spongelike or aerogel structure of carbon nanomaterials as an electrode and in situ synthesis of nanomaterials on the electrode surface. In this case, the durability of modified cathode electrodes could be improved. Third, considering the potential effects of leached carbon nanomaterials to the environment, nanomaterial leakage and its environmental toxicity also need to be systematically evaluated. Finally, there are many laboratory-scale researches on the application of modified cathodes with carbon nanomaterials in EF processes, but the industrial application of these cathodes is still not developed. More studies are needed to investigate the cost-effectiveness of large-scale modified cathode fabrication including the supply of carbon nanomaterials and to monitor the long-term stability of modified cathodes under practical application conditions.

Acknowledgment The authors thank the University of Tabriz (Iran) for all the support provided. We also acknowledge the support of Iran Science Elites Federation.

References

1. Brillas E, Sirés I, Oturan MA (2009) Electro-Fenton process and related electrochemical technologies based on fenton's reaction chemistry. Chem Rev 109(12):6570–6631
2. Nidheesh PV, Gandhimathi R (2012) Trends in electro-Fenton process for water and wastewater treatment: an overview. Desalination 299:1–15
3. Oloman C, Watkinson AP (1975) The electroreduction of oxygen to hydrogen peroxide on fluidized cathodes. Can J Chem Eng 53(3):268–273
4. Oloman C, Watkinson AP (1979) Hydrogen peroxide production in trickle-bed electrochemical reactors. J Appl Electrochem 9(1):117–123
5. Khataee AR, Safarpour M, Zarei M, Aber S (2011) Electrochemical generation of H_2O_2 using immobilized carbon nanotubes on graphite electrode fed with air: investigation of operational parameters. J Electroanal Chem 659(1):63–68

6. Scialdone O, Galia A, Sabatino S (2013) Electro-generation of H_2O_2 and abatement of organic pollutant in water by an electro-Fenton process in a microfluidic reactor. Electrochem Commun 26:45–47
7. Leng WH, Zhu WC, Ni J, Zhang Z, Zhang JQ, Cao CN (2006) Photoelectrocatalytic destruction of organics using TiO_2 as photoanode with simultaneous production of H_2O_2 at the cathode. Appl Catal A 300(1):24–35
8. Scialdone O, Galia A, Gattuso C, Sabatino S, Schiavo B (2015) Effect of air pressure on the electro-generation of H_2O_2 and the abatement of organic pollutants in water by electro-Fenton process. Electrochim Acta 182:775–780
9. Santana-Martínez G, Roa-Morales G, Martin del Campo E, Romero R, Frontana-Uribe BA, Natividad R (2016) Electro-Fenton and electro-Fenton-like with in situ electrogeneration of H_2O_2 and catalyst applied to 4-chlorophenol mineralization. Electrochim Acta 195:246–256
10. Flox C, Ammar S, Arias C, Brillas E, Vargas-Zavala AV, Abdelhedi R (2006) Electro-Fenton and photoelectro-Fenton degradation of indigo carmine in acidic aqueous medium. Appl Catal B 67(1-2):93–104
11. Liang L, An Y, Zhou M, Yu F, Liu M, Ren G (2016) Novel rolling-made gas-diffusion electrode loading trace transition metal for efficient heterogeneous electro-Fenton-like. J Environ Chem Eng 4(4):4400–4408
12. Wang Z-X, Li G, Yang F, Chen Y-L, Gao P (2011) Electro-Fenton degradation of cellulose using graphite/PTFE electrodes modified by 2-ethylanthraquinone. Carbohydr Polym 86 (4):1807–1813
13. Flores N, Cabot PL, Centellas F, Garrido JA, Rodríguez RM, Brillas E, Sirés I (2017) 4-Hydroxyphenylacetic acid oxidation in sulfate and real olive oil mill wastewater by electrochemical advanced processes with a boron-doped diamond anode. J Hazard Mater 321:566–575
14. Wang A, Qu J, Ru J, Liu H, Ge J (2005) Mineralization of an azo dye Acid Red 14 by electro-Fenton's reagent using an activated carbon fiber cathode. Dyes Pigments 65(3):227–233
15. Hammami S, Oturan N, Bellakhal N, Dachraoui M, Oturan MA (2007) Oxidative degradation of direct orange 61 by electro-Fenton process using a carbon felt electrode: application of the experimental design methodology. J Electroanal Chem 610(1):75–84
16. Pimentel M, Oturan N, Dezotti M, Oturan MA (2008) Phenol degradation by advanced electrochemical oxidation process electro-Fenton using a carbon felt cathode. Appl Catal B 83(1-2):140–149
17. Zhou M, Tan Q, Wang Q, Jiao Y, Oturan N, Oturan MA (2012) Degradation of organics in reverse osmosis concentrate by electro-Fenton process. J Hazard Mater 215-216:287–293
18. Zhou L, Zhou M, Zhang C, Jiang Y, Bi Z, Yang J (2013) Electro-Fenton degradation of p-nitrophenol using the anodized graphite felts. Chem Eng J 233:185–192
19. Yahya MS, Oturan N, El Kacemi K, El Karbane M, Aravindakumar CT, Oturan MA (2014) Oxidative degradation study on antimicrobial agent ciprofloxacin by electro-Fenton process: kinetics and oxidation products. Chemosphere 117:447–454
20. Özcan A, Şahin Y, Savaş Koparal A, Oturan MA (2008) Carbon sponge as a new cathode material for the electro-Fenton process: comparison with carbon felt cathode and application to degradation of synthetic dye basic blue 3 in aqueous medium. J Electroanal Chem 616 (1–2):71–78
21. Trellu C, Péchaud Y, Oturan N, Mousset E, Huguenot D, van Hullebusch ED, Esposito G, Oturan MA (2016) Comparative study on the removal of humic acids from drinking water by anodic oxidation and electro-Fenton processes: mineralization efficiency and modelling. Appl Catal B 194:32–41
22. Alvarez-Gallegos A, Pletcher D (1998) The removal of low level organics via hydrogen peroxide formed in a reticulated vitreous carbon cathode cell, part 1. The electrosynthesis of hydrogen peroxide in aqueous acidic solutions. Electrochim Acta 44(5):853–861

23. Alverez-Gallegos A, Pletcher D (1999) The removal of low level organics via hydrogen peroxide formed in a reticulated vitreous carbon cathode cell. Part 2: the removal of phenols and related compounds from aqueous effluents. Electrochim Acta 44(14):2483–2492
24. Martínez SS, Bahena CL (2009) Chlorbromuron urea herbicide removal by electro-Fenton reaction in aqueous effluents. Water Res 43(1):33–40
25. Thiam A, Sirés I, Garrido JA, Rodríguez RM, Brillas E (2015) Decolorization and mineralization of Allura Red AC aqueous solutions by electrochemical advanced oxidation processes. J Hazard Mater 290:34–42
26. Thiam A, Zhou M, Brillas E, Sirés I (2014) Two-step mineralization of Tartrazine solutions: study of parameters and by-products during the coupling of electrocoagulation with electrochemical advanced oxidation processes. Appl Catal B 150–151:116–125
27. Cruz-González K, Torres-Lopez O, García-León AM, Brillas E, Hernández-Ramírez A, Peralta-Hernández JM (2012) Optimization of electro-Fenton/BDD process for decolorization of a model azo dye wastewater by means of response surface methodology. Desalination 286:63–68
28. Cruz-González K, Torres-López O, García-León A, Guzmán-Mar JL, Reyes LH, Hernández-Ramírez A, Peralta-Hernández JM (2010) Determination of optimum operating parameters for Acid Yellow 36 decolorization by electro-Fenton process using BDD cathode. Chem Eng J 160(1):199–206
29. Su DS, Perathoner S, Centi G (2013) Nanocarbons for the development of advanced catalysts. Chem Rev 113(8):5782–5816
30. Hassani A, Khataee AR (2017) Activated carbon fiber for environmental protection. In: Chen JY (ed) Activated carbon fiber and textiles. Woodhead Publishing, Oxford, pp 245–280
31. Inagaki M, Kang F (2014) Fundamental science of carbon materials. Materials science and engineering of carbon: fundamentals2nd edn. Butterworth-Heinemann, Oxford, pp 17–217
32. Wei Q, Tong X, Zhang G, Qiao J, Gong Q, Sun S (2015) Nitrogen-doped carbon nanotube and graphene materials for oxygen reduction reactions. Catalysts 5(3):1574
33. Wang D-W, Su D (2014) Heterogeneous nanocarbon materials for oxygen reduction reaction. Energy Environ Sci 7(2):576–591
34. Mousset E, Ko ZT, Syafiq M, Wang Z, Lefebvre O (2016) Electrocatalytic activity enhancement of a graphene ink-coated carbon cloth cathode for oxidative treatment. Electrochim Acta 222:1628–1641
35. Ren W, Tang D, Lu X, Sun J, Li M, Qiu S, Fan D (2016) Novel multilayer ACF@rGO@OMC cathode composite with enhanced activity for electro-Fenton degradation of phthalic acid esters. Ind Eng Chem Res 55(42):11085–11096
36. Chen C-Y, Tang C, Wang H-F, Chen C-M, Zhang X, Huang X, Zhang Q (2016) Oxygen reduction reaction on graphene in an electro-Fenton system: in situ generation of H_2O_2 for the oxidation of organic compounds. ChemSusChem 9(10):1194–1199
37. Iijima S (1991) Helical microtubules of graphitic carbon. Nature 354(6348):56–58
38. Dai L, Xue Y, Qu L, Choi H-J, Baek J-B (2015) Metal-free catalysts for oxygen reduction reaction. Chem Rev 115(11):4823–4892
39. Popov VN (2004) Carbon nanotubes: properties and application. Mater Sci Eng R Rep 43 (3):61–102
40. Zhang X, Lei L, Xia B, Zhang Y, Fu J (2009) Oxidization of carbon nanotubes through hydroxyl radical induced by pulsed O_2 plasma and its application for O_2 reduction in electro-Fenton. Electrochim Acta 54(10):2810–2817
41. Tian J, Olajuyin AM, Mu T, Yang M, Xing J (2016) Efficient degradation of rhodamine B using modified graphite felt gas diffusion electrode by electro-Fenton process. Environ Sci Pollut Res 23(12):11574–11583
42. Chu Y, Zhang D, Liu L, Qian Y, Li L (2013) Electrochemical degradation of m-cresol using porous carbon-nanotube-containing cathode and Ti/SnO_2–Sb_2O_5–IrO_2 anode: kinetics, byproducts and biodegradability. J Hazard Mater 252-253:306–312

43. Khataee AR, Safarpour M, Zarei M, Aber S (2012) Combined heterogeneous and homogeneous photodegradation of a dye using immobilized TiO_2 nanophotocatalyst and modified graphite electrode with carbon nanotubes. J Mol Catal A Chem 363–364:58–68
44. Khataee AR, Vahid B, Behjati B, Safarpour M, Joo SW (2014) Kinetic modeling of a triarylmethane dye decolorization by photoelectro-Fenton process in a recirculating system: nonlinear regression analysis. Chem Eng Res Des 92(2):362–367
45. Khataee AR, Vahid B, Behjati B, Safarpour M (2013) Treatment of a dye solution using photoelectro-fenton process on the cathode containing carbon nanotubes under recirculation mode: investigation of operational parameters and artificial neural network modeling. Environ Prog Sustain Energy 32(3):557–563
46. Pajootan E, Arami M, Rahimdokht M (2014) Discoloration of wastewater in a continuous electro-Fenton process using modified graphite electrode with multi-walled carbon nanotubes/surfactant. Sep Purif Technol 130:34–44
47. Es'haghzade Z, Pajootan E, Bahrami H, Arami M (2017) Facile synthesis of Fe_3O_4 nanoparticles via aqueous based electro chemical route for heterogeneous electro-Fenton removal of azo dyes. J Taiwan Inst Chem Eng 7:91–105
48. Fu J, Zhang X, Lei L (2007) Fe-modified multi-walled carbon nanotube electrode for production of hydrogen peroxide. Acta Phys Chim Sin 23(8):1157–1162
49. Tang Q, Wang D, Yao DM, Yang CW, Sun YC (2016) Highly efficient electro-generation of hydrogen peroxide using NCNT/NF/CNT air diffusion electrode for electro-Fenton degradation of p-nitrophenol. Water Sci Technol 73(7):1652–1658
50. Babaei-Sati R, Basiri Parsa J (2017) Electrogeneration of H_2O_2 using graphite cathode modified with electrochemically synthesized polypyrrole/MWCNT nanocomposite for electro-Fenton process. J Ind Eng Chem 52:270–276
51. Zhang X, Fu J, Zhang Y, Lei L (2008) A nitrogen functionalized carbon nanotube cathode for highly efficient electrocatalytic generation of H_2O_2 in electro-Fenton system. Sep Purif Technol 64(1):116–123
52. Zarei M, Salari D, Niaei A, Khataee AR (2009) Peroxi-coagulation degradation of C.I. Basic Yellow 2 based on carbon-PTFE and carbon nanotube-PTFE electrodes as cathode. Electrochim Acta 54(26):6651–6660
53. Zarei M, Niaei A, Salari D, Khataee AR (2010) Application of response surface methodology for optimization of peroxi-coagulation of textile dye solution using carbon nanotube–PTFE cathode. J Hazard Mater 173(1–3):544–551
54. Zarei M, Khataee AR, Ordikhani-Seyedlar R, Fathinia M (2010) Photoelectro-Fenton combined with photocatalytic process for degradation of an azo dye using supported TiO_2 nanoparticles and carbon nanotube cathode: neural network modeling. Electrochim Acta 55 (24):7259–7265
55. Geim AK, Novoselov KS (2007) The rise of graphene. Nat Mater 6(3):183–191
56. Kiew SF, Kiew LV, Lee HB, Imae T, Chung LY (2016) Assessing biocompatibility of graphene oxide-based nanocarriers: a review. J Control Release 226:217–228
57. Novoselov KS, Geim AK, Morozov SV, Jiang D, Zhang Y, Dubonos SV, Grigorieva IV, Firsov AA (2004) Electric field effect in atomically thin carbon films. Science 306 (5696):666–669
58. Lee C, Wei X, Kysar JW, Hone J (2008) Measurement of the elastic properties and intrinsic strength of monolayer graphene. Science 321(5887):385–388
59. Balandin AA, Ghosh S, Bao W, Calizo I, Teweldebrhan D, Miao F, Lau CN (2008) Superior thermal conductivity of single-layer graphene. Nano Lett 8(3):902–907
60. Marinho B, Ghislandi M, Tkalya E, Koning CE, de With G (2012) Electrical conductivity of compacts of graphene, multi-wall carbon nanotubes, carbon black, and graphite powder. Powder Technol 221:351–358
61. Novoselov KS (2009) Graphene: the magic of flat carbon. ECS Trans 19(5):3–7
62. Chen D, Tang L, Li J (2010) Graphene-based materials in electrochemistry. Chem Soc Rev 39 (8):3157–3180

63. Lee HC, Liu W-W, Chai S-P, Mohamed AR, Lai CW, Khe C-S, Voon CH, Hashim U, Hidayah NMS (2016) Synthesis of single-layer graphene: a review of recent development. Proc Chem 19:916–921
64. Shao G, Lu Y, Wu F, Yang C, Zeng F, Wu Q (2012) Graphene oxide: the mechanisms of oxidation and exfoliation. J Mater Sci 47(10):4400–4409
65. Perreault F, Fonseca de Faria A, Elimelech M (2015) Environmental applications of graphene-based nanomaterials. Chem Soc Rev 44(16):5861–5896
66. Liu L, Qing M, Wang Y, Chen S (2015) Defects in graphene: generation, healing, and their effects on the properties of graphene: a review. J Mater Sci Technol 31(6):599–606
67. Xu X, Chen J, Zhang G, Song Y, Yang F (2014) Homogeneous electro-Fenton oxidative degradation of reactive brilliant blue using a graphene doped gas-diffusion cathode. Int J Electrochem Sci 9:569–579
68. Le TXH, Bechelany M, Lacour S, Oturan N, Oturan MA, Cretin M (2015) High removal efficiency of dye pollutants by electron-Fenton process using a graphene based cathode. Carbon 94:1003–1011
69. Le TXH, Bechelany M, Champavert J, Cretin M (2015) A highly active based graphene cathode for the electro-Fenton reaction. RSC Adv 5(53):42536–42539
70. Zhao F, Liu L, Yang F, Ren N (2013) E-Fenton degradation of MB during filtration with Gr/PPy modified membrane cathode. Chem Eng J 230:491–498
71. Dong H, Su H, Chen Z, Yu H, Yu H (2016) Fabrication of electrochemically reduced graphene oxide modified gas diffusion electrode for in-situ electrochemical advanced oxidation process under mild conditions. Electrochim Acta 222:1501–1509
72. Shen J, Li Y, Zhu Y, Hu Y, Li C (2016) Aerosol synthesis of graphene-Fe_3O_4 hollow hybrid microspheres for heterogeneous Fenton and electro-Fenton reaction. J Environ Chem Eng 4 (2):2469–2476
73. Zhao X, Liu S, Huang Y (2016) Removing organic contaminants by an electro-Fenton system constructed with graphene cathode. Toxicol Environ Chem 98(3-4):530–539
74. Zhang Z, Zhang J, Ye X, Hu Y, Chen Y (2016) Pd/RGO modified carbon felt cathode for electro-Fenton removing of EDTA-Ni. Water Sci Technol 74(3):639–646
75. Zhang G, Zhou Y, Yang F (2015) FeOOH-catalyzed heterogeneous electro-Fenton system upon anthraquinone@graphene nanohybrid cathode in a divided electrolytic cell: catholyte-regulated catalytic oxidation performance and mechanism. J Electrochem Soc 162(6):H357–H365
76. Mousset E, Wang Z, Hammaker J, Lefebvre O (2016) Physico-chemical properties of pristine graphene and its performance as electrode material for electro-Fenton treatment of wastewater. Electrochim Acta 214:217–230
77. Liu T, Wang K, Song S, Brouzgou A, Tsiakaras P, Wang Y (2016) New electro-Fenton gas diffusion cathode based on nitrogen-doped graphene@carbon nanotube composite materials. Electrochim Acta 194:228–238
78. Li Y, Han J, Xie B, Li Y, Zhan S, Tian Y (2017) Synergistic degradation of antimicrobial agent ciprofloxacin in water by using 3D CeO_2/RGO composite as cathode in electro-Fenton system. J Electroanal Chem 784:6–12
79. Li Y, Li Y, Xie B, Han J, Zhan S, Tian Y (2017) Efficient mineralization of ciprofloxacin using a 3D $Ce_xZr_{1-x}O_2$/RGO composite cathode. Environ Sci Nano 4(2):425–436
80. Govindaraj D, Nambi IM, Senthilnathan J (2017) An innate quinone functionalized electrochemically exfoliated graphene/Fe_3O_4 composite electrode for the continuous generation of reactive oxygen species. Chem Eng J 316:964–977
81. Golabi SM, Raoof JB (1996) Catalysis of dioxygen reduction to hydrogen peroxide at the surface of carbon paste electrodes modified by 1,4-naphthoquinone and some of its derivatives. J Electroanal Chem 416(1):75–82
82. Jürmann G, Schiffrin DJ, Tammeveski K (2007) The pH-dependence of oxygen reduction on quinone-modified glassy carbon electrodes. Electrochim Acta 53(2):390–399

83. Walcarius A (2013) Mesoporous materials and electrochemistry. Chem Soc Rev 42 (9):4098–4140
84. Sun M-H, Huang S-Z, Chen L-H, Li Y, Yang X-Y, Yuan Z-Y, Su B-L (2016) Applications of hierarchically structured porous materials from energy storage and conversion, catalysis, photocatalysis, adsorption, separation, and sensing to biomedicine. Chem Soc Rev 45 (12):3479–3563
85. Hu J, Sun J, Yan J, Lv K, Zhong C, Deng K, Li J (2013) A novel efficient electrode material: activated carbon fibers grafted by ordered mesoporous carbon. Electrochem Commun 28:67–70
86. Peng Q, Zhang Z, Za H, Ren W, Sun J (2014) N-doped ordered mesoporous carbon grafted onto activated carbon fibre composites with enhanced activity for the electro-Fenton degradation of Brilliant Red X3B dye. RSC Adv 4(104):60168–60175
87. Ren W, Peng Q, Huang Z, Zhang Z, Zhan W, Lv K, Sun J (2015) Effect of pore structure on the electro-Fenton activity of ACF@OMC cathode. Ind Eng Chem Res 54(34):8492–8499
88. Liu Y, Chen S, Quan X, Yu H, Zhao H, Zhang Y (2015) Efficient mineralization of perfluorooctanoate by electro-Fenton with H_2O_2 electro-generated on hierarchically porous carbon. Environ Sci Technol 49(22):13528–13533
89. Wang Y, Liu Y, X-Z L, Zeng F, Liu H (2013) A highly-ordered porous carbon material based cathode for energy-efficient electro-Fenton process. Sep Purif Technol 106:32–37
90. Chen W, Yang X, Huang J, Zhu Y, Zhou Y, Yao Y, Li C (2016) Iron oxide containing graphene/carbon nanotube based carbon aerogel as an efficient E-Fenton cathode for the degradation of methyl blue. Electrochim Acta 200:75–83
91. Perazzolo V, Durante C, Gennaro A (2016) Nitrogen and sulfur doped mesoporous carbon cathodes for water treatment. J Electroanal Chem 782:264–269
92. Perazzolo V, Durante C, Pilot R, Paduano A, Zheng J, Rizzi GA, Martucci A, Granozzi G, Gennaro A (2015) Nitrogen and sulfur doped mesoporous carbon as metal-free electrocatalysts for the in situ production of hydrogen peroxide. Carbon 95:949–963
93. Liu Y, Quan X, Fan X, Wang H, Chen S (2015) High-yield electrosynthesis of hydrogen peroxide from oxygen reduction by hierarchically porous carbon. Angew Chem 127(23):6941–6945